https://doi.org/10.15255/KUI.2021.047
KUI-16/2022
Original scientific paper
Received June 27, 2021
Accepted September 19, 2021

Effect of Synthesis Methods on the Catalytic Reforming of Kerosene

E. Saidi,[a] *M. Ziarati*,[a*] *H. Dehghani*,[a] and *N. Khandan*[b]

[a] Malek Ashtar University of Technology, Faculty of Chemistry and Chemical Engineering, Iran
[b] Iranian Research Organization for Science & Technology (IROST), Department of Chemical Technologies, Iran

Abstract

Ni/Y samples were prepared by various synthesis methods to investigate the catalyst performance in the reforming of kerosene. Properties of the samples were characterised using XRD, BET, NH_3-TPD, and FTIR techniques. Analysis of the products revealed that more isoalkanes were obtained by the sol-gel method (37.3 %), but the deposition method produced higher aromatic content (32.7 %). Ultimately, the production of 75.81 % jet fuel with a standard range of aromatics (10.70 %) and higher naphthenes (19.3 %) over impregnated catalyst led us to conclude that lower Brønsted acid sites inhibited the occurrence of side reactions and produced more jet fuels.

Keywords

Reforming, kerosene, synthesis method, Ni/Y catalysts, zeolite

1 Introduction

Catalytic reforming of hydrocarbons over zeolites is a promising way to produce various oil-based fuels.[1,2] Small-size catalysts are used to prepare high external surface of the crystals, which can then convert large molecules and prevent deactivation.[3] While most bifunctional catalysts in recent studies have been prepared by one preparation method, different preparation methods of catalysts tend to influence their behaviour during the process as well as the properties of the produced fuels.[4,5] Various parameters such as pH, reaction temperature, reaction time, and type of solvent are important in obtaining a ceramic powder with the desired shape and size.[6] Therefore, synthetic strategies of catalysts are important in a chemical process, and catalyst preparation is known as the main path to a desired activity and selectivity.[7,8] In the literature, there are various methods to incorporate metal into the support. Impregnation (dry or wet), ion exchange, co-precipitation, deposition–precipitation (DP), and sol–gel (SG) are among the most conventional methods of catalyst preparation deserving particular attention.[9,10] Each preparation method has advantages and disadvantages.[4] For instance, deposition–precipitation and sol-gel methods are among the most common techniques applied to synthesize the nanoparticles. Proper metal dispersion is achievable by the sol-gel method. However, this method is usually not applicable to high metal loading due to the agglomeration of particles .[11] On the other hand, the impregnation (IM) method is a simple way to economically produce metal particles with larger sizes and higher Si/Al ratios. This method can be applied in cases of high metal loading.[12] The mechanism of reforming process is shown as follows.

$$\text{alkane} \xrightarrow{\text{Lewis acid}} \text{carbonium ion} \xrightarrow{\text{Brønsted acid}} \text{olefin} \xrightarrow{\text{Brønsted acid}} \text{oligomer} \xrightarrow{\text{Brønsted acid}} \text{naphthenes} \xrightarrow{\text{Lewis acid}} \text{aromatic}$$

According to this mechanism, both Lewis and Brønsted acid sites advance the reforming process.[4] Metals play the role of Lewis acid sites, and the supports provide the Brønsted acid sites. Therefore, the incorporation of the metals into the catalysts is needed to enhance the chemicals in these types of processes.[13] The support porosity also affects metal dispersion and particle size.[14] Y zeolites, one of many zeolites applied to this process, have been used as the main active component in FCC catalysts in the last half–century (since the 1960's), due to their higher pore volume and pore size, shorter length of channels, and larger external surface area than other zeolites.[15,16] Alternatively, nickel (Ni), with its lower cost, greater availability, higher activity, and extensive application in hydrocarbon reforming, is mostly used together with the Y zeolite.[17–20] However, there are only rare reports about comparative studies on Ni/Y catalysts prepared by different methods.

Catalytic reforming of kerosene is an important process because it is applied in the production of many kinds of jet fuels. The base of some trade fuels, like Jet–A1, and most applicable jet propellants, such as JP–8 and JP–5, is kerosene.[21] All of these fuels contain four main hydrocarbon components, namely, normal alkanes, isoalkanes, naphthenes, and aromatics.[22] In the present study, reforming of kerosene was performed over Ni/Y samples prepared using various synthetic procedures. Several physicochemical properties of the prepared Ni/Y samples were characterised to investigate the effect of each synthetic method on the catalytic performance in the reforming process. Furthermore, the results of the liquid analysis were interoperated to introduce a favourable preparation method to produce desired fuel.

* Corresponding author: Mahmoud Ziarati, PhD
Email: maziarati@mut.ac.ir

2 Experimental

2.1 Materials

Nickel nitrate hexahydrate ($Ni(NO_3)_2 \cdot 6H_2O$) and sodium carbonate (Na_2CO_3) were purchased from the Merck Company (Germany), and commercial Y zeolite (Si/Al = 5.1 in Na-form, surface area 900 $m^2 g^{-1}$) was supplied by the Zeolyst Company (USA). Kerosene was supplied by the Tehran Oil Refinery Company (TORC, Iran), the properties of which are reported in Table 1.

Table 1 – Specifications of kerosene supplied by TORC

Property	ASTM Test method	Specification limit	Feed properties
Density at 15.6 °C / kg m^{-3}	D 4052	775.0–840.0 min-max	797.4
Distillation IBP %VOL at 185 °C %VOL at 200 °C %VOL at 210 °C %VOL at 235 °C FBP	D 86	 REP. °C REP. % Vol. REP. % Vol. REP. % Vol. REP. % Vol. 300 °C	 156 23.9 48.4 % 64.1 % 90.9 % 260
Sulphur	D 1552	wt.%	0.09
Flash point	D 3828	38 °C min	50
Freezing point	D 2386	−47 °C max	−52
Acidity	D 3242	% VOL	0.5 ml/0.5 ml
Aromatic content	D 6379	% VOL	21.3 %

2.2 Catalyst preparation

2.2.1 Deposition- precipitation method

To prepare a 10 % Ni/NaY sample by the deposition-precipitation method, appropriate weights of 1 M nickel nitrate ($Ni(NO_3)_2 \cdot 6H_2O$) and Na_2CO_3 solutions were added simultaneously to deionised water at 70 °C with continuous stirring at 500–700 rpm, and a low flow rate of basic Na_2CO_3 solution (1 ml min^{-1}) to control the pH around 7 ± 0.2. After ageing under slower stirring (300 rpm) and filtration, the sample was washed three times with deionised water at 70 °C and added to a suspension of NaY. The mixtures were stirred (300–500 rpm), filtered, and dried in two steps: firstly, sample temperature was increased from an ambient temperature to 90 °C over 2 h, then further increased to 110 °C, and maintained at this temperature in air overnight; secondly, it was calcined in a kiln with a preliminary temperature of 150 °C in three steps: 1) the sample was heated at 150 °C for 10 min, 2) the temperature was increased from 150 to 550 °C in airflow at a rate of 5 °C min^{-1}, and 3) the temperature was maintained at 550 °C for 4 h. The catalyst so prepared was designated Ni/NaY–DP.

2.2.2 Impregnation method

In this method, a certain amount of metal in an aqueous solution of nickel nitrate was added to the zeolite, and then dried and calcined to achieve the desired loading. The wetness impregnation procedure, similar to the one described in the literature, was applied to synthesize the catalyst.[8] For this purpose, $Ni(NO_3)_2 \cdot 6H_2O$ was firstly poured into deionised water. Subsequently, the NaY zeolite was added to the solution and stirred at 300–500 rpm at ambient temperature, and then dried in an oven at 110 °C for 12 h. Finally, the catalyst was calcined in air at 550 °C at a heating rate of 5 °C min^{-1} for 4 h. The catalyst so prepared was designated Ni/NaY–IM.

2.2.3 Sol–gel method

In this method, $Ni(NO_3)_2 \cdot 6H_2O$ and Y zeolite in a stoichiometric ratio required for 10 % Ni/NaY were added to deionised water, and citric acid was then poured into the prepared aqueous solution to chelate Ni^{2+}. As mentioned in previous works, the amount of citric acid added was two times the metal moles to obtain the sol by continuous stirring.[23] The gel was obtained by slowly evaporating the sol at 70 °C over 2 h, and then heating it to 110 °C and maintained at this temperature overnight. Finally, the samples were annealed at 550 °C for 4 h. The catalyst so prepared was designated Ni/NaY–SG.

2.3 Catalyst characterisation

In this research, various techniques were applied to characterise physical, chemical, and structural elements of the prepared Ni/Y samples. X–ray powder diffraction (XRD) patterns were recorded on a Philips PW-3710 X–ray diffractometer using a Cu Ka source (λ = 1.5418°A) in the angle range of 2θ between 5° to 80° with Cu–Kα radiation at a rate of 2° min^{-1}. To identify the diffraction patterns, they were compared with those of a known structure in the Joint Committee of Powder Diffraction Standards (JCPDS) database.

The surface area of the fresh catalysts was calculated from a Nitrogen Physisorption analysis on a CHEMBET-3000 surface characterisation analyser (Quantachrome Instruments Company) operating at –77 K. Total surface area was determined by the Brunauer–Emmett–Teller (BET) equation using relative pressure (P/P_0) ranging from 0.005 to 0.1, and the t-plot method was applied to survey microporous characteristics.

Fourier transform infrared spectroscopy (FTIR) using a Thermo Nicolet Nexus Model was applied to study the distribution of Brønsted and Lewis acid sites in the samples. At first, a wafer was prepared to perform pyridine adsorption. It was then heated at 350 °C in a vacuum and cooled to ambient temperature. Physisorbed pyridine was degassed at 150 °C for 1 h in a vacuum, and removed. Finally, the FTIR spectra were prepared. The concentration of acid sites was determined from the peak area at 1455 cm^{-1} for Lewis acid sites and 1545 cm^{-1} for Brønsted acid sites.[24]

Temperature programmed desorption of ammonia (NH_3–TPD) equipped with a thermal conductivity detector (TCD) was employed using a BELCAT-M instrument (BEL Japan

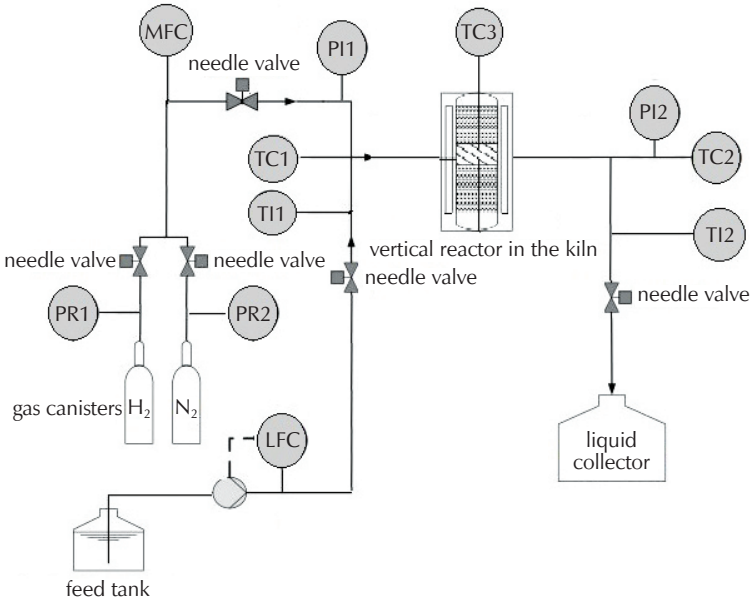

Fig. 1 – Schematic of the experimental setup used in this research, where LFC – liquid flow controller; MFC – mass flow controller; pump–peristaltic pump; TC – thermocouple; TI – temperature indicator; PI – pressure indicator; PR – pressure regulator

Inc.) to determine acidity of the zeolites and prepared catalysts. Profiles of NH_3–TPD were obtained at a temperature ranging from 50 to 550 °C at a constant heating rate of 10 °C min^{-1} in a 40 ml min^{-1} flow of helium.

2.4 Catalytic reforming process

The reaction was carried out in a stainless steel fixed-bed reactor with an inner diameter of 10 mm (ID = 10 mm) and a length of 150 mm at 450 °C and atmospheric pressure. For each test, the reactant kerosene was fed by controlling its flow rate in the setup, as shown in Fig. 1.

In the first step of the reforming process, 1 g powdery catalyst, sizes between 20–40 mesh, was uniformly packed into the reactor tube, which occupied approximately 1 cm of the reactor height. To place the catalyst into the reactor, a metal sieve was applied as a bed in the middle of a vertical reactor. The tubular reactor was placed into a vertical kiln. This kiln provided energy to reach this endothermic process to the considered reaction temperature (450 °C). The void space before the catalyst bed inside the reactor facilitated the heat transfer and increased the temperature to 450 °C. To eliminate oxygen, the system was purged by N_2 flow for 10 min under 70 cc min^{-1} before the reaction. The catalyst was then reduced in pure hydrogen at 300 °C for 4 h with a flow rate of 50 ml min^{-1}. The feed was injected to the system by the TEC1 peristaltic pump (AQUA, Italy) at a flow rate of 5 ml min^{-1}. It was heated to 300 °C by a preheater before entering the reactor. The reaction temperature was increased to 450 °C by the reactor heating system, and the reaction was carried out at 450 °C. Finally, liquid products were collected for analysis using two-step traps.

The analysis of liquid products was carried out using an Agilent 6890N gas chromatography (GC) equipped with a DH capillary column (40 m) and flame ionization detector (FID). In this way, a standard solution of normal alkanes (200 ppm) in n-hexane (C6) as a solvent, was used. The injection temperature was set to 300 °C. The column temperature was initially increased from 40 to 100 °C (heating rate of 2 °C min^{-1}), and then increased to 300 °C (heating rate of 10 °C min^{-1}), and maintained for 8 min.

3 Results and discussion

3.1 Results of the textural properties

The XRD patterns for the prepared samples are displayed in Fig. 2.

The prepared catalysts clearly displayed the characteristic XRD patterns of Y structure. Therefore, the zeolite framework was well maintained after incorporating the Ni, but its crystallinity had slightly changed by the synthesis. The formation of a cubic phase in NiO (JCPDS Card 47–1049) with a lattice constant, a = 4.1771 Å had shown in XRD pattern, where distinct peaks at 2θ of 37.26°, 43.29°, 62.88°, 75.42°, and 79.41° were identified as peaks of cubic NiO crystals with various diffraction planes of (111), (200), (220), (311), and (222), respectively.[25]

According to the literature, a reduction in Ni/Y samples generates a metal phase. It creates particle growth, which leads to the formation of larger metal crystallites supported

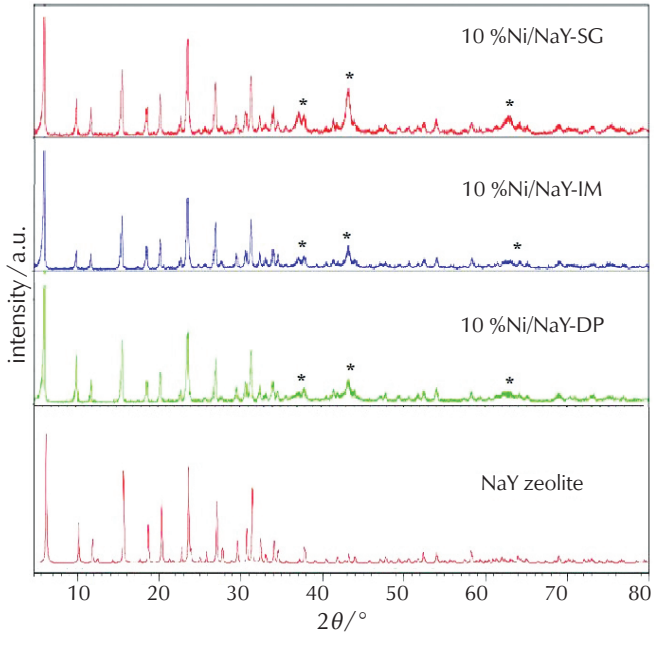

Fig. 2 – XRD patterns of NaY zeolite and prepared samples

Table 2 – Textural properties of Ni/Y samples

Row	Sample	Surface area / $m^2\,g^{-1}$			Pore volume / $cm^3\,g^{-1}$		
		BET[a]	Micropore[b]	External	Total	Micropore[b]	Mesopore
1	Ni/Y-DP	580	475	362	0.45	0.16	0.31
2	Ni/Y-SG	627	521	394	0.51	0.29	0.21
3	Ni/Y-IM	490	383	163	0.39	0.14	0.12

[a] Calculated by BET method, [b] t-Plot method, [c] volume at $P/P_0 = 0.99$

on the outer surface.[26] However, not all the peaks were distinguished in this study, as some particle sizes were below the XRD detection limit. The distinct peaks at 2θ of 37.26°, 43.29°, and 62.88° for the NiO crystals are identified with an asterisks in Fig. 2. As shown in Eq. 1, the average crystal size of different phases was calculated from the XRD results using the Debye-Scherer equation.[27]

$$D = \frac{\kappa\lambda}{\beta\cos\theta} \tag{1}$$

where $k = 0.89$, λ is the wavelength of Cu-Kα radiations, β is the full width at half maximum (FWHM), and θ is the angle obtained from 2θ values corresponding to maximum intensity peak in the XRD pattern. In general, there is a direct relationship between the peak breadths of a specific phase of material to the mean crystallite size of that material.[28] According to the results of the Scherer equation, the calculated size for nickel oxide nanoparticles for catalysts prepared by sol-gel, deposition-precipitation, and impregnation methods were 6.988, 8.986, and 10.483, respectively. In this result, the NiO was crystalline.

The results of the surface areas and pore volumes of Y zeolites and Ni/Y catalysts are indicated in Table 2.

Ni loading was 9.5, 10.2, and 9.8 for the DP, SG, and IM methods, respectively, which are close to expected amounts. Based on the characterisation results, all samples had a large surface area and good characterisations, such as small crystallite size.

3.2 Acidity characterisation

Py-FTIR using a Thermo Nicolet Nexus Model was applied to study the distribution of Brønsted and Lewis acid sites in the samples. Firstly, a wafer was prepared to perform pyridine adsorption. The wafer was then heated at 350 °C in a vacuum and cooled to ambient temperature. Physisorbed pyridine was then degassed at 150 °C for 1 h in a vacuum, and removed to achieve the FTIR spectra. As shown in Fig. 3, the concentration of acid sites was obtained from the peak area at 1455 cm^{-1} for Lewis, and 1545 cm^{-1} for Brønsted acid sites.[24]

The IR bands found at 1544, 1490, and 1455 cm^{-1} correspond to the Brønsted acid sites (B), the total acidity (B+L), and the Lewis acid sites (L), respectively. The introduction of NiO particles into NaY zeolite by impregnation (IM) decreased the Brønsted acidity, whereas intensity was high

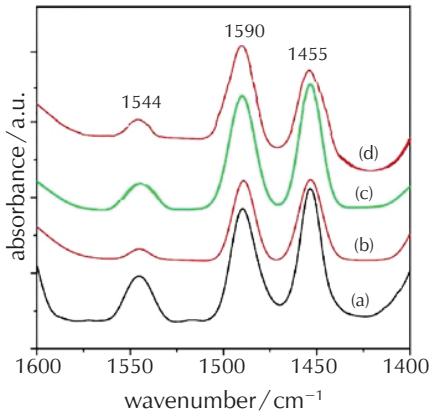

Fig. 3 – FTIR spectra of (a) NaY, (b) 10 % Ni/Y-IM, (c) 10 % Ni/NaY-SG, and (d) 10 % Ni/NaY-DP

in the SG and DP samples. The reason for the reduction in Brønsted acidity was the lower crystallinity of the impregnated sample (as shown by XRD and BET results) and the occupation of NiO particles on the Brønsted sites. On the other hand, an increase in Lewis acidity was observed after adding NiO particles. Ni/Y-SG had the highest B/L ratio (0.29); Ni/Y-DP showed a relatively moderate B/L ratio (0.25), and Ni/Y-IM had a lower B/L ratio (0.10). For the NH_3-TPD analysis, each sample was initially degassed by 50 ml min^{-1} helium (He) at 550 °C for 2 h. The sample was then cooled to 100 °C and treated with a 5 mol% flow of NH_3 gas (balanced by He) for 1 h. This was followed by a He flow for 1 h to remove residual NH_3. Finally, the sample was heated to 700 °C at 10 °C min^{-1} in a continuous flow of helium. The results of acidity in the case of Y zeolites and Ni/Y catalysts were obtained by NH_3-TPD analysis, and are indicated in Table 3 and Fig. 4.

As mentioned in the literature, there are three classifications according to the ammonia desorption temperature for the strength of acid sites. The acidity is usually classified in ranges of 100–250 °C, 250–400 °C, and 400–550 °C for better interpretation of acid sites in TPD-NH_3 analysis, which correspond to weak, medium, and strong acid sites, respectively.[29] According to previous studies, the change in the Si/Al ratio in the catalysts prepared by different methods is minimal. Therefore, the reason to have a different acidity profile is to modify the NiO. When NiO was modified, some of the acid sites of the zeolite Y were covered in NiO particles. The NiO introduces medium-strength acidity onto the zeolite support.[6] As observed in Fig. 4, weak acid sites outnumbered strong acid sites in all the samples.

Table 3 – Acidity of the catalysts synthesised by different methods

Row	Sample	NH_3-TPD acidity / mmol g^{-1}				Py-FTIR acidity / mmol g^{-1} (at 200 °C)			
		Weak	Medium	Strong	Total	Brønsted (B)	Lewis (L)	Total acid (B + L)	B/L Ratio
1	Ni/Y-DP	0.61	1.86	1.95	4.42	0.38	1.53	1.94	0.25
2	Ni/Y-SG	1.03	1.51	2.07	4.61	0.49	1.68	2.17	0.29
3	Ni/Y-IM	1.12	0.89	1.12	3.13	0.12	1.15	1.41	0.10

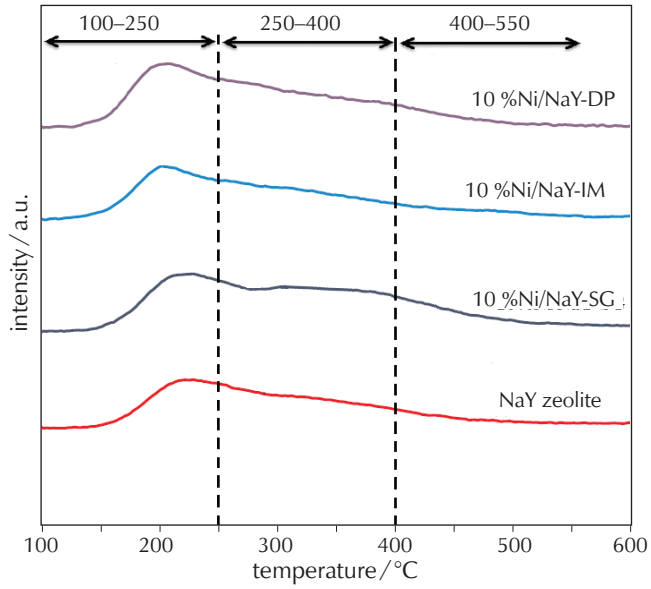

Fig. 4 – Profiles of NH_3-TPD for NaY zeolite and the prepared catalysts

However, the impregnated sample showed significantly fewer medium and strong acid sites, while the sol-gel sample had more strong acid sites than the other samples.

3.3 Catalyst deactivation discussion

Two problems in the catalytic works are reactivation by coke and sintering. Coke formation in the reforming of hydrocarbons often occurs at temperature above 600 °C. On the other hand, the reaction temperature was 450 °C, which was lower than critical reaction (600 °C) for coke formation.

Sintering of Ni often occurs above 600 °C; the reaction temperature (450 °C) was lower than this temperature. Besides, the XRD of the used catalysts showed low probability of sintering. This, the deactivation of the catalysts would not occur in this research.

3.4 Component analysis of the products

Table 4 shows the analysis of reaction products in terms of four main components, normal alkanes, isoalkanes, naphthenes, and aromatics over the prepared Ni/Y catalysts.

Based on the observed and previously reported results, it can be concluded that reforming over catalysts prepared using the DP and IM methods produced lighter liquid products than those prepared by the SG method. As a result, catalysts prepared by the DP method produced the highest aromatic contents in comparison to the IM or SG methods. This was due to the suitable ratio of Lewis and low Brønsted acid sites, which led to progress in the reforming process. In fact, according to the mechanism of reaction, the Lewis acids convert alkanes to carbonium ions. Then, the Brønsted acid sites create olefins, oligomers and naphthenes (cycloparaffins), respectively. Finally, the Lewis acid sites convert naphthenes to aromatics.[30] Therefore, the existence of a suitable proportion of both sites is necessary for the progress of the process.

The prepared catalysts converted the components of kerosene to other types of hydrocarbons. The Ni/NaY-SG catalyst showed higher isoalkanes compared to the same catalysts prepared by other methods. The selectivity in siting and particle size of metal within the zeolite cage structure were the two main parameters that affected the activity of this catalyst. The preparation step could place the metal atoms into the main channel of the zeolites or in the super cages during the preparation method. Metal ions may migrate to smaller cages of zeolites by removing water during

Table 4 – Results of hydrocarbon contents of produced liquids (wt. %)

Row	Catalyst	Method	Alkanes	Isoalkanes	Naphthenes	Aromatic
1	Fresh feed	---	27.4	27.9	23.5	21.2
2	10 % Ni/NaY	DP	54.3	10	3.4	32.3
3	10 % Ni/NaY	IM	35.6	34.6	19.2	10.6
4	10 % Ni/NaY	SG	32.3	37.3	3	27.4

Table 5 – Results of the product distribution in reforming process

Row	Sample	IBP/°C	EBP/°C	Gasoline (C5–C10)	Jet fuel (C9–C15)	Diesel (C14–C20)	Lubricant (C19–C25)
1	Ni/Y-DP	160	283	10.56 %	86.91 %	2.53 %	0
2	Ni/Y-IM	162	285	22.05 %	75.81 %	2.14 %	0
3	Ni/Y-SG	158	296	19.48 %	77.61 %	2.76 %	0.15 %

calcination. Impregnated samples with lower conversions of naphthenes and higher conversions of aromatics produce a proper liquid. This product meets the requirements of jet fuels with carbon contents of C8 to C18 and aromatic contents of 10.6 %; the aromatic limitation is often less than 25 %. This may be due to its larger particle size, which acts selectively by allowing the aromatic components of the feedstock to pass through it during the reforming process. Another reason is the decrease in crystallinity, indicated by XRD, which causes lower IM catalyst activity, and advances the reaction towards more naphthenic production.[1]

3.5 Catalytic performance of the samples

The hydrocarbons are categorised by their carbon chain length into gasoline (C5–C10), jet fuel (C9–C15), diesel (C14–C20), and lubricant (C19–C25).[31,32] The product distribution of product compositions (%) over all samples in the reforming process is presented in Table 5.

According to Table 5, the liquid product by the DP method contained 10.56 % gasoline, 86.91 % jet fuel, and 2.53 % diesel hydrocarbon. The ranges of products over the IM catalyst were 22.05 % gasoline, 75.81 % jet fuel, and 2.14 % diesel. In the case of the sol-gel method, 19.48 % gasoline, 77.61 % jet fuel, 2.76 % diesel, and 0.15 % lubricant were produced. All catalysts indicated high performance, which was attributed to the intrinsic structure of the Y zeolite with high crystallinity, and a high concentration of strong acid sites on its surface.

Both sol-gel and wetness impregnation methods improved the formation of isoalkanes. However, the hydrocarbon ranges of liquid produced over Ni/NaY-SG was C8 to C25, which indicated the production of heavier hydrocarbons than Ni/NaY-IM (C8 to C18) and Ni/NaY- DP (C8 to C17). One reason may be the greater activity of the metal particles anchored to the outer surface area; these sites were far more predominant when metal was deposited by impregnation.[23] The high gasoline content over the IM catalyst was due to more Brønsted acid sites, which helped the reforming process to produce lighter components. This is in line with the mechanism of cracking reaction, which needs Brønsted acid sites to advance the reaction towards more production of naphthenic components. Table 6 presents the results of product compositions over the three prepared catalysts.

Table 6 – Results of product compositions in reforming process

Row	Distilled product	Compositions of products	Ni/Y-DP	Ni/Y-IM	Ni/Y-SG
1	Gasoline (C5–C10)	Alkanes	5.00 %	26.13 %	42.73 %
		Isoalkanes	54.59 %	39.96%	41.78 %
		Naphthenes	24.79 %	25.99 %	7.75 %
		Aromatics	15.62 %	31.42 %	7.74 %
2	Jet fuel (C9–C15)	Alkanes	53.95 %	35.13 %	31.84 %
		Isoalkanes	10.12 %	34.87 %	37.46 %
		Naphthenes	3.01 %	19.30 %	3.45 %
		Aromatics	32.92 %	10.70 %	27.25 %
3	Diesel (C14–C20)	Alkanes	22.9 %	23.14 %	12.42 %
		Isoalkanes	38.49 %	41.38 %	23.98 %
		Naphthenes	0	0	0
		Aromatics	38.62 %	35.48 %	63.60 %
4	Lubricant (C19–C25)	Alkanes	0	0	100.00 %
		Isoalkanes	0	0	0
		Naphthenes	0	0	0
		Aromatics	0	0	0

According to the data in Table 6, as the acidity of the catalyst increased, conversion to naphthenic components decreased. Therefore, the amount of naphthenes produced over an impregnated catalyst with the lowest acidity and highest B/L ratio was higher than with others.

As these results reveal, the sol-gel method produced only a few liquids (0.15 %) with carbon numbers in the range of lubricants. In addition, all compositions of the products were normal alkanes in this range. Hence, this product has not the specification of a normal lubricant. As a result, no significant change in molecular weight distribution occurred in the reforming process, and compositions of all products were in the ranges of feedstock. The deposition-precipitation method showed enhanced capability for jet fuel production, while the impregnated sample produced more carbon chains in the range of gasoline. However, the hydrocarbons in the range of jet fuels produced over impregnated catalysts with higher naphthenes were of higher quality due to the higher energy content of these compositions.

4 Conclusions

Ni/Y catalysts were successfully synthesized through conventional preparation methods, and the effect of key parameters on their catalytic performance was investigated during the reforming process. Kerosene was applied as the feedstock (with 27.4 % normal alkanes, 27.9 % isoalkanes, 23.5 % naphthenes, and 21.2 % aromatics), the content of which was then changed during the reforming process. The results showed that acid sites of the Y zeolites would consequently affect its catalytic performance in the reforming process. One of the main reasons for the production of higher products was the content of Brønsted acid sites in the catalyst. In this research, the catalyst synthesized by the SG method had Brønsted acid sites, which was due to the effect of its solvent on their acid sites. However, an increase in the B/L ratio decreased the naphthenic content, and as a result, degraded the quality of the prepared jet fuels. Although less jet fuel was produced over the catalyst prepared by the IM method (75.81 %), this fuel was of higher quality due to its allowable aromatics and high amount of naphthenes, which were related to the fewer Brønsted acid sites of this catalyst.

ACKNOWLEDGEMENTS

The financial support by Malek Ashtar University of Technology is highly appreciated.

References
Literatura

1. *F. Zaera*, Selectivity in hydrocarbon catalytic reforming: a surface chemistry perspective, Appl. Catal. A. **229** (2002) 75–91, doi: https://doi.org/10.1016/S0926-860X(02)00017-0.
2. *E. Aghaei, R. Karimzadeh, H. R. Godini, A. Gurlo, O. Gorke*, Improving the physicochemical properties of Y zeolite for catalytic cracking of heavy oil via sequential steam-alkali-acid treatments, Microporous Mesoporous Mater. **294** (2020) 109854, doi: https://doi.org/10.1016/j.micromeso.2019.109854.
3. *X. Su, W. Zan, X. Bai, G. Wang, W. Wu*, Synthesis of microscale and nanoscale ZSM-5 zeolites: effect of particle size and acidity of Zn modified ZSM-5 zeolites on aromatization performance, Catal. Sci. Technol. **7** (2017) 1943–1952, doi: https://doi.org/10.1039/C7CY00435D.
4. *M. Y. Choo, L. E. Oi, T. J. Daou, T. C. Ling, Y. C. Lin, G. Centi, E. P. Ng, J. C. Juan*, Deposition of NiO nanoparticles on nanosized zeolite NaY for production of biofuel via hydrogen-free deoxygenation, Materials **13** (2020) 3104, doi: https://doi:10.3390/ma13143104.
5. *N. N. Marei, N. N. Nassar, G. Vitale*, The effect of the nanosize on surface properties of NiO nanoparticles for the adsorption of quinolin-65. Phys. Chem. Chem. Phys. **18** (2016) 6839–6849, doi: https://doi.org/10.1039/C6CP00001K.
6. *A. Rajaeiyan, M. M. Bagheri-Mohagheghi*, Comparison of sol-gel and co-precipitation methods on the structural properties and phase transformation of γ and α-Al_2O_3 nanoparticles, Adv. Manuf. **1** (2013) 176–182, doi: https://doi.org/10.1007/s40436-013-0018-1.
7. *Y. Wang, O. V. Kikhtyanin, C. Li, X. Su, X. Bai, W. Wu*, Synthesis of nanosized ZSM-5 zeolites by different methods and their catalytic performance in the alkylation of naphthalene, Pet. Chem. **61** (2021) 394–406, doi: https://doi.org/10.1134/S0965544121030087.
8. *G. Ertl, H. Knozinger, J. Weitkamp*, Preparation of solid catalysts. New York, Wiley, 1999.
9. *V. M. Akhmedov, S. H. Al-Khowaiter, J. K. Al-Refai*, Hydroconversion of C5–C8 alkanes over Zr-containing supported catalysts prepared by metal vapor method, Appl. Catal. A **252** (2003) 353–361, doi: https://doi.org/10.1016/S0926-860X(03)00496-4.
10. *A. Masalska, J. R. Grzechowiak, K. Jaroszewska*, Effect of metal-support interactions in Ni/ZSM-5 + Al_2O_3 catalysts on the transformation of n-Paraffins, Top Catal. **56** (2013) 981–994, doi: https://doi.org/10.1007/s11244-013-0062-x.
11. *M. A. Cauqui, J. M. Rodriguezizquierdo*, Application of the Sol-gel methods to catalyst preparation, J. Non-Cryst. Solids **147** (1992) 724–738, doi: https://doi.org/10.1016/S0022-3093(05)80707-0.
12. *P. Yan, J. Mensah, A. Adesina, E. Kennedy, M. Stockenhuber*, Highly-dispersed Ni on BEA catalyst prepared by ion-exchange-deposition precipitation for improved hydrodeoxygenation activity, Appl. Catal. B. Environ. **267** (2020) 118690, doi: https://doi.org/10.1016/j.apcatb.2020.118690.
13. *K. Akubo, M. A. Nahil, P. T. Williams*, Aromatic fuel oils produced from the pyrolysis-catalysis of polyethylene plastic with metal-impregnated zeolite catalysts, J. Energy Inst. **92** (2019) 195–202, doi: https://doi.org/10.1016/j.joei.2017.10.009.
14. *D. P. Gamliel, B. P. Baillie, E. Augustine, J. Hall, G. M. Bollas, J. A. Valla*, Nickel impregnated mesoporous USY zeolites for hydrodeoxygenation of anisole. Microporous Mesoporous Mater. **261** (2018) 18–28 doi: https://doi.org/10.1016/j.micromeso.2017.10.027.
15. *T. Wada, K. I. Kaneda, S. Murata, M. Nomura*, Effect of modifier Pd metal on hydrocracking of polyaromatic compounds over Ni-loaded Y-type zeolite and its application as hydrodesulfurization catalyst, Catal. Today **3** (1996) 113–120, doi: https://doi.org/10.1016/0920-5861(96)00023-5.
16. *S. Suganuma, N. Katada*, Innovation of catalytic technology for upgrading of crude oil in petroleum refinery, Fuel Process Technol. **208** (2020) 106518, doi: https://doi.org/10.1016/j.fuproc.2020.106518.
17. *D. Yao, H. Yang, H. Chena, P. T. Williams*, Investigation of nickel-impregnated zeolite catalysts for hydrogen/syngas production from the catalytic reforming of waste polyethylene, Appl. Catal. B. Environ. **227** (2018) 477–487, doi: https://doi.org/10.1016/j.apcatb.2018.01.050.
18. *X. Yang, J. Da, H. Yu, H. Wang*, Characterization and performance evaluation of Ni-based catalysts with Ce promoter for methane and hydrocarbons steam reforming process, Fuel **179** (2016) 353–361, doi: https://doi.org/10.1016/j.fuel.2016.03.104.
19. *D. Karthikeyan, N. Lingappan, B. Sivasankar*, Hydroisomerization of *n*-Octane over bifunctional Ni−Pd/HY zeolite catalysts, Ind. Eng. Chem. Res. **47** (2008) 6538–6546, doi: https://doi.org/10.1021/ie7017299.
20. *N. Chang, Z. Gu, Z. Wang*, Study of Y zeolite catalysts for coal tar hydro-cracking in supercritical gasoline, J. Porous. Mater. **18** (2011) 289–596, doi: https://doi.org/10.1007/s10934-010-9413-1.
21. *S. Parkash*, Petroleum Fuels manufacturing handbook including specialty products and sustainable manufacturing techniques, The McGraw-Hill companies, Inc., New York, Chicago, San Francisco, Lisbon, London, Madrid, Mexico City, Milan, New Delhi, San Juan, Seoul, Singapore, Sydney, Toronto, 2010.

22. *H. Ruan, Y. Qin, J. Heyne, R. Gieleciak, M. Fenga, B. Yang*, Chemical compositions and properties of lignin-based jet fuel range hydrocarbons, Fuel **256** (2019) 115947, doi: https://doi.org/10.1016/j.fuel.2019.115947.
23. *J. Wang, Y. Liu, M. Zhang, Y. Qiao, T. Xia*, Comparison of the sol-gel method with the coprecipitation technique for preparation of hexagonal barium ferrite, Chem. Res. Chinese Universities **24** (2008) 525–528, doi: https://doi.org/10.1016/S1005-9040(08)60110-5.
24. *H. Coqueblin, A. Richard, D. Uzio, L. Pinarda, Y. Pouilloux, F. Epron*, Effect of the metal promoter on the performances of H-ZSM5 in ethylene aromatization, Catal. Today **289** (2016) 62–69, doi: https://doi.org/10.1016/j.cattod.2016.08.006.
25. *C. Baerlocher, L. B. McCusker, D. H. Olson*, Atlas of zeolite framework types, Elsevier, Amsterdam, 2007.
26. *A. Lucas, A. Garrido, P. Sánchez, A. Romero, J. L. Valverde*, Growth of Carbon Nanofibers from Ni/Y Zeolite Based Catalysts: Effects of Ni introduction method, reaction temperature, and reaction gas composition, Ind. Eng. Chem. Res. **44** (2005) 8225–8236, doi: https://doi.org/10.1021/ie058027k.
27. *P. Gaurh, H. Pramanik*, *In-situ* production of valuable aromatics via pyrolysis of waste polypropylene using commercial catalyst ZSM-5, Indian J. Chem. Technol. **27** (2020) 144–152, url: http://14.139.47.23/index.php/IJCT/article/viewFile/23613/465477728.
28. *T. Theivasanthi, M. Alagar*, An Insight Analysis of Nano sized powder of jackfruit seed, Nano Biomed. Eng. **3** (2011) 163–168, doi: https://doi.org/10.5101/nbe.v3i3.p163-168.
29. *A. Akah, C. Colin, G. Arthur*, The selective catalytic oxidation of NH_3 over Fe-ZSM-5, Appl. Catal. B. Environ. **59** (2005) 221–226, doi: https://doi.org/10.1016/j.apcatb.2004.10.020.
30. *S. Lycourghiotis, E. Kordouli, L. Sygellou, K. Bourikas, C. Kordulis*, Nickel catalysts supported on palygorskite for transformation of waste cooking oils into green diesel, Appl. Catal. B Environ. **259** (2019) 118059, doi: https://doi.org/10.1016/j.apcatb.2019.118059.
31. *T. K. Habibie, B. H. Susanto, M. F. Carli*, Effect of NiMo/zeolite catalyst preparation method for bio jet fuel synthesis, E3S Web of Conferences (2018), doi: https://doi.org/10.1051/e3sconf/20186702024.
32. *L. Chen, X. Wang, H. Guo, X. Guo, Y. Wang, H. Liu, G. Li*, Hydroconversion of *n*-octane over nanoscale HZSM-5 zeolites promoted by 12-molybdophosphoric acid and Ni, Catal. Commun. **8** (2007) 416–423, doi: https://doi.org/10.1016/j.catcom.2006.06.034.

SAŽETAK

Utjecaj metode sinteze na katalitičko reformiranje kerozina

Elham Saidi,[a] *Mahmoud Ziarati*,[a*] *Hossein Dehghani*[a] i *Nahid Khandan*[b]

Uzorci Ni/Y pripremljeni su različitim metodama sinteze da bi se ispitala učinkovitost katalitičkog reformiranja kerozina. Svojstva uzoraka karakterizirana su tehnikama XRD, BET, NH_3-TPD i FTIR. Utvrđeno je da je više izoalkana nastaje sol-gel metodom (37,3 %), dok se metodom deponiranja dobiva veći udio aromata (32,7 %). Proizvodnja 75,81 % mlaznog goriva standardnog udjela aromata (10,70 %) i viših naftena (19,3 %) na impregniranom katalizatoru rezultirala je zaključkom da manji broj Bronstedovih kiselinskih mjesta koči pojavu usporednih reakcija te nastaje više mlaznog goriva.

Ključne riječi
Reformiranje, kerozin, metoda sinteze, Ni/Y katalizatori, zeolit

[a] *Malek Ashtar University of Technology, Faculty of Chemistry and Chemical Engineering, Iran*
[b] *Iranian Research Organization for Science & Technology (IROST), Department of Chemical Technologies, Iran*

Izvorni znanstveni rad
Prispjelo 27. lipnja 2021.
Prihvaćeno 19. rujna 2021.